MICHIGAN STATE UNIVERSITY

CYCLOTRON LABORATORY

TWO-FLUID HYDRODYNAMICS APPLIED TO THE DECONFINEMENT TRANSITION IN THE FRAGMENTATION REGION IN ULTRA-RELATIVISTIC NUCLEAR COLLISIONS

H.W. BARZ, B. KÄMPFER, L.P. CSERNAI, B. LUKÁCS

OCTOBER 1986

MSUCL-577

MSUCL-#577
October 1986

Two-Fluid Hydrodynamics Applied to the Deconfinement Transition in the Fragmentation Region in Ultra-Relativistic Nuclear Collisions

H.W. Barz and B. Kämpfer

Central Institute for Nuclear Research Rossendorf,
PF 19, Dresden, 8051, GDR

L.P. Csernai*

National Superconducting Cyclotron Laboratory
Michigan State University, East Lansing, MI 48824-1321, USA

B. Lukács

Central Institute of Physics Budapest
H-1125 Budapest, P.O.B. 49, Hungary

Abstract

A two-fluid model is presented which describes the interpenetration of nuclei colliding at ultra-relativistic energies. The two fluids are coupled by friction resulting from hadron-hadron collisions. The model calculations predict the deconfinement transition in the baryon-rich fragmentation region. The degree of the conversion and the maximum temperature depend sensitively on the characteristic time for the arrangement of nuclear matter into the quark gluon plasma.

1. Introduction

Heavy ions colliding with ultra-relativistic energies (E/A>10 GeV) are expected to penetrate one another. During this process they become highly excited and their decay products populate the fragmentation region, while in the central midrapidity region mostly mesons can be found. In this work we address the question whether sufficient energy can be stored in the excited nuclei to produce a quark-gluon plasma as it is predicted by the quantum chromodynamics (see e.g.[1]).

The energy density of the matter in the fragmentation region was first estimated in ref. 2, and a sufficiently high energy density for the deconfinement transition was found. This energy stems from the captured secondary particles which emerge in the elementary hadron-hadron interactions. The compression arises from the fact that the nucleons at the front of the target are struck earlier than the nucleons at the back side. Detailed hydrodynamical calculations were carried out first in ref. 3. In these calculations, it was assumed that the matter arises from materializing color fields, which were created by the colliding target and projectile nucleons. This picture implies a violation of the baryon number conservation immediately after the collision and causes a relatively moderate increase of the nucleon density. This point was extensively analyzed in ref. 4 where the importance of the details of the recoil mechanism for the final baryon and energy density was stressed. In ref. 4 the evolution of the target region is described under the influence of the color electric field in an ultra-relativistic approximation. The strength of the color field increases with the mass of the projectile and was adjusted to experiment by the requirement that the target nucleons obtain the same amount of rapidity as the protons lose in p+A reactions[5,6].

We intend now to study the target fragmentation region within a two-fluid model. The two fluids representing the target and the projectile interact with each other. Such an approach was already applied[7] to collisions of heavy ions at energies below 2 GeV·A, where the thermalization of the initial two-fluid components into one is close to complete. Therefore in this energy region, the simpler one-fluid model can compete with the two-fluid description. At higher bombarding energies the velocities of the two fluids remain high enough to distinguish them from each other. However, now the deceleration of the projectile and target are not treated independently, unlike in the ultra-relativistic treatment.[4] So, our treatment bridges the gap between the two energy regimes and is able to explore the lower limit for the ultra-relativistic scenario.

Furthermore, to investigate the possibility of a phase transition we use an equation of state which allows the nuclear matter to undergo the deconfinement transition to a quark-gluon plasma. The time of this transition plays an important role. Since estimates of the transition time vary between 1 fm/c[8] and 0.1 fm/c[9], and are rather uncertain, we discuss our results as a function of this transition time.

In sec. 2 we present the two-fluid model. It is applied to symmetric slab on slab collisions in sec. 3. In sec. 4 the results are discussed and our conclusions can be found in sec. 5.

2. Two-fluid model

We describe the two nuclei as two perfect fluids. The energy momentum tensor, e.g. of the target nucleus is

$$T^{ij} = (e+p)u^i u^j + pg^{ij}. \qquad (2.1)$$

Here e and p stand for the energy density and the pressure, and u^i means the flow velocity $u^i=(\gamma,\gamma v)$, where $\gamma=(1-v^2)^{-1/2}$ is the Lorentz factor. We use the metric tensor $g^{ik}=(-1,1,1,1)$, thus $u^i u_i=-1$. It is provided that the difference of the flow velocities of the target and the projectile fluid components remains high enough compared to the thermal velocity of the hadrons inside the fluid to prevent hadrons scattering from one fluid component to the other. Therefore the baryon number densities satisfy the equations of continuity

$$(nu^i)_{,i} = 0,$$
$$(\bar{n}\bar{u}^i)_{,i} = 0, \tag{2.2}$$

where quantities belonging to the projectile fluid are barred to distinguish them from those of the target fluid. The hydrodynamic equations of motion of one isolated fluid are $T^{ik}{}_{,k}=0$. In our case both fluids interact and exchange energy and momentum due to the elementary hadron-hadron collisions. This fact is expressed by the coupling of the equations of motion. In the following we restrict us to a local scalar coupling

$$T^{ij}{}_{,j} = -Dn\bar{n}(u^i-\bar{u}^i),$$
$$\bar{T}^{ij}{}_{,j} = -Dn\bar{n}(\bar{u}^i-u^i). \tag{2.3}$$

Due to the local coupling assumption, the friction function D is nonvanishing only in the region where the two fluids overlap. Such a coupling was used in describing conventional heavy ion reactions in ref. 7

and can be derived from a relativistic Boltzmann equation. Nonlocal interactions arising from the chromoelectric field, which become important at ultrarelativistic energies[4] are not considered. The special form of the coupling term has the consequence that the sum of both energy momentum tensors is converted, i.e. $(T^{ij} + \bar{T}^{ij})_{,j}=0$. That means that the energy distributed in the elementary hadron-hadron collisions remains inside the fluids. This assumption cannot be kept at ultra-relativistic energies because the finite materialization time in connection with the Lorentz dilation converts a considerable amount of energy into color fields. Correspondingly in (2.3) we also neglect the energy gain by the materialization of the color fields. If the nuclei would stop on top of each other, both effects will roughly compensate. However, as the nuclei traverse, we overestimate the energy of the fragmentation region by the amount of energy deposited in the midrapidity region. This limits the applicability of the model to not too high energies. An improvement would require the introduction of a nonlocal interaction similar to that used in ref. 4 in the ultra-relativistic regime.

In ref. 10 an expression for the coupling strength D was derived from the relativistic Boltzmann equation for the case when the elastic hadron-hadron scattering dominates. Then D is related to the loss of the longitudinal momentum of the nucleon by

$$D = \frac{1}{2}\left(\frac{s}{s-4m^2}\right)^{1/2} \sigma_{el}/Bm \ . \qquad (2.4)$$

Here s is the square of the c.m. energy in a nucleon-nucleon collision, m the nucleon mass and the differential cross sections are parametrized as

$d\sigma_{el}/dt \sim e^{Bt}$ ($B=8$ GeV^{-2}), where t is the square of the transferred four momentum.

Since at high energies the inelastic processes dominate, we add a term: $\sigma_{inel}\ m\ \Delta y$ to eq. (2.4). The momentum-loss can be estimated from the measured inelastic cross sections. Assume two nucleons with initial rapidities 0 and y which, after their collision, gain rapidities Δy and $y-\Delta y$, while the secondaries are distributed in the midrapidity region with a constant rapidity density dN/dy. These particles are overwhelmingly pions with a transverse mass of $m_t \approx 0.4$ GeV. From the energy conservation requirement we obtain $\Delta y \approx m_t \langle N \rangle / y \cdot m$ in a rather good approximation. Taking the experimental data we find that Δy is a slowly increasing function of energy which saturates at 1.2. The analysis[11] of the rapidity distribution of the leading proton of the recent p+A experiments[5,6] is consistent with a rapidity loss of

$$\langle \Delta y \rangle_n = 1 + (n-1)/\alpha, \quad \alpha = 3 \pm 1$$

after n inelastic collisions.

This expression shows us that the secondary collisions are less violent than the first one. For heavy nuclei a mean rapidity loss of $\Delta y = 0.4$ per collision can be deduced, which provides us with the coupling

$$D = \sigma_{in}\ m\Delta y = 1.2 \text{ GeV fm}^2. \tag{2.5}$$

Besides this value we shall also use an energy dependent coupling which follows from eq. (2.4) and the above estimate of the inelastic part together with the pp-data[12]

$$D = (2.3 - 3.3/\ell n\ s + 0.8/\ell^2 n\ s)\text{GeV fm}^2 \tag{2.6}$$

One should have in mind that the estimate of D is rather uncertain. Namely, after the front particles have collided, the following ones hit already excited nucleons and matter, so the quantities σ_{in}, m and Δy may have changed. E.g. Clare and Strottman[13] proposed an essentially larger value of D.

Now, we have to specify the equation of state. We assume that the matter consists of a mixture of the normal nuclear matter phase and a plasma phase as in earlier works[14,15]. For the nuclear matter phase we use a quadratic approximation for the compression energy and the thermal energy of a Boltzmann gas

$$e = mn + \frac{K}{18}\, n(n/n_0 - 1)^2 + \frac{3}{2}\, Tn + \frac{\pi^2}{10}\, T^4, \tag{2.7}$$

where n_0 denotes the normal nuclear matter density of 0.16 fm^{-3}, T is the temperature and the incompressibility is chosen to be K = 280 MeV. The last term in eq. (2.7) takes into account the pions in a high temperature approximation. The eq. (2.7) reflects important features of nuclear matter (see e.g. ref. 16) and is sufficient for our exploratory investigations. To complete the equations of state we take the nucleonic entropy similar to that of the Boltzmann gas plus the pionic component,

$$s = \frac{5}{2}\, n + n\ \ell n \left\{ \frac{4}{n} \left(\frac{mT}{2\pi\hbar^2} \right)^{3/2} \right\} + \frac{4\pi^2}{30}\, T^3 \ . \tag{2.8}$$

The plasma state of the matter is modelled by a noninteracting gas of light quarks and gluons. Using the thermodynamical potential

$$p(\mu,T) = -B + \frac{37}{90}\pi^2T^4 + \mu^2T^2 + \frac{\pi^2}{2}\mu^4 \ , \tag{2.9}$$

the entropy $s=\partial p/\partial T$ and the particle number density $n=\partial p/\partial \mu$ can be derived as a function of the temperature and the chemical potential μ. For the bag constant a value of $B^{1/4}$=235 MeV is used. If the system has time enough to equilibrate, the Gibbs conditions for pressure, temperature and chemical potential

$$p_{nm} = p_{qm}, \quad T_{nm} = T_{qm}, \quad \mu_{nm} = 3\mu_{qm} \tag{2.10}$$

hold. From these conditions a phase diagram arises which is shown in fig. 2. The hatched area indicates the region, where both phases coexist.

In our dynamical treatment we drop the last condition in eq. (2.10), assuming that the matter is in mechanical and thermal equilibrium but not in chemical equilibrium. Then we introduce the progress variable x, in addition to the thermodynamic variables n and T, by

$$x = \frac{N_1}{N_1+N_2} \ . \tag{2.11}$$

This quantity denotes the ratio of the number of baryons in the nuclear matter phase, N_1, to the total baryon number, $N_1 + N_2$. In equilibrium this ratio $x_{eq}(n,T)$ is a unique function of n and T. In the non-equilibrium this ratio deviates from the equilibrium value and approaches it in a relaxation process. For this process we use[15] a linearized form

$$\dot{x} = -(x - x_{eq})/\tau \ , \tag{2.12}$$

where τ is the relaxation time measured in the local rest frame. The QCD scale suggest that τ lies in the order of $\hbar/B^{1/4} \sim 1$ fm/c. Since reliable estimates are still outstanding (see e.g. refs. 8 and 9), we vary τ in the range between 0.1 fm/c and 1 fm/c.

3. Numerical treatment of the hydrodynamical equations

To reduce the numerical expense we solve the hydrodynamical equations in one dimension. Thus, we represent the nuclei by two slabs having a finite thickness. Furthermore, we consider symmetric target and projectile combinations. Then in the center-of-mass system the mirror symmetry is preserved between the target and the projectile fluid

$$\bar{u}^0(t,x) = u^0(t,-x)$$
$$\bar{u}^1(t,x) = -u^1(t,-x) \ . \tag{3.1}$$

Thus it is sufficient to treat from eqs. (2.3) and (2.4) only the equations for the target fluid.

We introduce a Lagrangian coordinate system τ,ξ which moves with the flow velocity $u^i=\gamma(1,v)$ in the center-of-mass system. Such a system can be obtained from the coordinate transformation $t=\tau$ and $x=x(\tau,\xi)$. Then the line element in the Minkowski space $ds=-dt^2+dx^2$ reads

$$ds^2 = -(1-\dot{x}^2)d\tau^2 + 2\dot{x}\, x'\, d\tau d\xi + x'^2 d\xi^2, \tag{3.2}$$

where $\dot{x} = \partial\chi(\tau,\xi)/\partial\tau$ and $x' = \partial x(\tau,\xi)/\partial\xi$. Identifying the flow velocity with $\dot{x}$

$$v = \frac{u^1}{u^0} = \frac{\partial x(\xi,\tau)}{\partial \tau} \tag{3.3}$$

the fluid velocity in the comoving system vanishes as required. Using this transformation, the continuity relation (2.2) can be written as

$$\frac{\partial}{\partial \tau} (\gamma n \frac{\partial x}{\partial \xi}) = 0 \ . \tag{3.4}$$

Projecting the equation of motion (2.3) on u^i we obtain the change of intrinsic energy

$$\gamma \frac{\partial}{\partial \tau} (\frac{e}{n}) + p\gamma \frac{\partial}{\partial \tau} (\frac{1}{n}) = -D\bar{n}(1+\bar{u}^i u_i) \tag{3.5}$$

and from the component i=1 we obtain the equation for the momentum change of a fluid element

$$\gamma \frac{\partial}{\partial \tau} (\frac{e+p}{n} u^1) = - \frac{1}{n} \frac{\partial p}{\partial x} - D\bar{n}(u^1-\bar{u}^1). \tag{3.6}$$

To treat the system of eqs. (3.3)-(3.6) numerically we divide the target fluid into cells which are labelled by the comoving coordinate $\xi = x(\xi, \tau=0)$. Then the equations are solved by following the motion of the cells using the fact that the comoving derivative is given by

$$\frac{\partial}{\partial \tau} = \frac{\partial}{\partial t} + v \frac{\partial}{\partial x} \ . \tag{3.7}$$

in the c.m. coordinates x,t. This always allows the use of the symmetry relations (3.1).

These equations determine the evolution of the needed quantities in the cm coordinates x and t: eq. (3.3) determines the new position of the cell labelled by ξ, eq. (3.4) fixes its density, eq. (3.5) prescribes the energy (or temperature) and eq. (3.6) gives the new velocity. For numerical calculation, the equations are discretized in accordance with the cell structure starting with a guess for u^i the consecutive application of the eqs. (3.3)-(3.6) defines an iterative procedure for the determination of u^i and the other quantities.

From eq. (3.5) it follows that the increase of the intrinsic energy of the target fluid is caused not only by the work of the pressure but also by energy transfer from the projectile fluid. In a microscopic picture the latter part may be viewed as an excitation of the colliding nuclei by hadron-hadron collisions and pion creation. This is in contrast to the model of ref. 4 where during the acceleration the color electric field does not increase directly the intrinsic energy.

The intrinsic energy is increased at the neutralization of the color fields, when these fields hadronize, and the created hadrons form an equilibrated fluid with the matter already present. Therefore, in ref. 4 the energy deposition is delayed and redistributed into the midrapidity region, as it is appropriate at asymptoticly high ultrarelativistic energies.

In the present model the energy and momentum deposition is simultaneous and happens locally. The created secondary hadrons are not separated from the target and projectile matter. Thus this model is applicable as long as the baryon force region has not yet been formed.

4. Results

The calculations are carried out for a slab thickness of d=10.6 fm corresponding to a collision of two heavy nuclei with mass numbers of $A \approx d^3 n_0 \approx 190$. In fig. 1 we show the results of the calculations for a bombarding energy of E/A = 10 GeV corresponding to a rapidity of $y_{lab}=3.15$. The calculations carried out in the cm system have been transformed to the target frame. The resulting phenomenon is a shock wave like behavior of the matter. There is some similarity to the "passing shock" model described in ref. 17. Behind the thin projectile with a lab thickness of $L/\cosh(y_{lab}) \approx 1$ fm the matter is compressed and moves with a rapidity of 0.9. But at the front of slab after the projectile has passed the matter expands and the density diminishes rapidly. For the transformation time $\tau=0.1$ fm/c maximum 80% of the matter is transformed into quark matter. The target velocity in the cm system is v=0.25 for the friction constant D=1.2 GeV fm^2 and v=0.45 when using eq. (2.6). Whereas the first value lies clearly below the thermal velocity the latter is already in the order of the thermal velocity. That means that the lower limit of the validity of our model is about 10 GeV per nucleon. At lower energies the formation of a third thermalized fluid component[7,18] should also be considered.

In fig. 2 we compare the evolution of the matter in the density temperature plane for different bombarding energies and transformation times. Fig. 2a shows the paths for a relaxation time of $\tau=1$ fm/c. As soon as the path reaches the hatched area of the coexistence region, the transformation into the quark gluon plasma starts and the slope of the trajectory diminishes due to the consumption of latent heat. However the transformation rate is slow compared to the rate of the penetration. Therefore the system becomes strongly overheated and for high bombarding energies high temperatures are attained. These high temperatures achieved

should not be taken too literally since we included only a very simple equation of state for the hadronic matter. In a more refined treatment, the inclusion of the full spectrum of hadronic resonances would strongly reduce these temperatures of overheated hadron matter.

For 10 GeV/nucleon beam energy, the rehadronization starts at the beginning of the expansion phase. At the higher bombarding energies of 40 and 160 GeV/nucleon, the transformation into the quark phase continues in the expansion stage until the coexistence region is reached. Then the rehadronization process sets in with a temperature near the critical temperature of the phase transition. At this stage a small reheating of the matter is observed. For the given three bombarding energies, only a partial transformation into quark matter (up to 85%) is reached because the phase transition is too slow compared to the dynamics of the flow.

Fig. 2b demonstrates the situation for a fast phase transition using τ=0.1 fm/c. Due to the fast consumption of the latent heat in forming the quark matter, the obtained densities and temperatures are much smaller than in the previous case. At the turning point of the trajectories for all three energies 85% of the baryons are dissolved into quarks and gluons. Except for E/A=10 GeV the transformation is completed during the expansion stage because the matter is excited highly enough. Later the rehadronization sets in and the paths follow again the lower borderlines of the coexistence region up to complete conversion into hadrons and breakup.

The maximal energy density reached in the course of the reaction is shown in fig. 3. The assumption of a constant coupling strength, eq. (2.5), gives a slightly higher energy density for small bombarding energies than the estimate eq. (2.6). This relation is reversed for high energies. In view of our previous discussion, the high energy densities may be

overestimated because we assumed a local interaction of the fluids which neglects the lead-out of energy into the mid-rapidity region. However, for the constant value of D, (eq. (2.5)), roughly the same energy densities are attained as in ref. 4 while for D according to eq. (2.6) a steep increase of excitation energy is predicted for E/A>100 GeV.

In contrast to the one-dimensional one-fluid model, in the two-fluid model the total energy of the system is not completely transformed into internal energy. A large amount of the energy remains as translational energy of the traversing nuclei. In fig. 4 we have represented the fraction of the energy which is transformed into internal energy of the fragmentation region. Furthermore, we have found that the rapidity loss of the projectile increases from 0.9 to 1.5 for bombarding energies ranging from 10 to 160 GeV. This result is only moderately dependent on the assumptions of the coupling strength D.

The dependence of the attained particle number and energy densities on the thickness of the two slabs is shown in fig. 5 for different bombarding energies. Whereas the energy density increases strongly the particle number density grows moderately. When increasing the energy the particle number density even decreases. For d=15 fm the matter of the two slabs still thermalize at 20 GeV.

5. Conclusions

If we intend to describe ultrarelativistic heavy ion reactions in the framework of fluid dynamics, the two-fluid model has to replace the one-fluid model at some bombarding energy E^*/A. Our model calculations indicate that the transition to the transparency of colliding nuclei occurs at bombarding energies $E^*_{stick}/A \gtrsim 10$ GeV. This value is not very sharply

defined and it depends on the assumption on the friction function D describing the interaction of the interpenetrating nuclei.

The obtained baryon densities are always considerably lower than the ones predicted by the one-fluid model (see e.g. ref. 14)). One simple reason lies in the fact that the densities do not sum up in the overlap region because a local equilibration cannot take place in the short time of contact. Nevertheless we obtain in our approach a sufficiently large energy density which allows the transition to a baryon rich plasma in the fragmentation region. In particular, if the critical energy density does not exceed essentially 2 GeV fm^{-3}, our model gives good reasons to predict the deconfinement in the fragmentation region. Higher energy densities are obtained only in case of a stronger interaction of the interpenetrating fluids as estimated by eq. (2.5), or for very high bombarding energies E/A ~ GeV. But in the latter energy region our model is not applicable in its present form with local interaction. Therefore, our results have to be supported by taking into account a more refined coupling between the two-fluids and the rising color fields as well as the quark-gluon plasma.

An important consequence of the two-fluid model is that the transformation time of the phase transition becomes crucial. For a moderate transformation time of τ=1 fm/c a complete phase transition is not reached. Roughly 85% of the matter can be transformed during the reaction. This amount should be still sufficient for observing the effects of the phase transition, however, the admixture of hadrons tends to wash out some signals of the plasma formation.

Otherwise, the mixture of highly excited hadron matter and plasma might lead to novel flow or fluctuation phenomena which distinguish themselves from the conventional effects in ordinary hadron matter. In this respect it

is worthwhile investigating the expansion of the excited fragment region more carefully. Steps in this direction have been performed in refs.19 and 20. If the breakup condition is reached at relatively high temperature this would show up in a large transverse momentum of the secondaries. A three-dimensional treatment is needed to estimate more quantitatively this effect.

This work is supported in part by the National Science Foundation under grant PHY 83-12245.

References

* On leave from the Central Research Inst. for Physics, Budapest, Hungary

1. K. Kajantie (ed.), Quark matter '84, Lecture Notes In Phys. 221 (1985), Springer-Verlag
2. R. Anishetti, P. Koehler and L. McLerran, Phys. Rev. D22 (1980) 2793
3. K. Kajantie, R. Raitio and V. Ruuskanen, Nucl. Phys. B222 (1983) 152
4. M. Gyulassy and L.P. Csernai, report LBL-20610, to be published
5. A. Barton et al., Phys. REv. D27 (1983) 2580
6. R.J. Ledoux et al., Proc. of XIV. Workshop of Gross Properties of Nuclei and Nucl. Excitation, Hirschegg, Austria, 1986
7. A. Amsden, A. Goldhaber, F. Harlow and J. Nix, Phys. Rev. C17 (1977) 2080
8. B. Müller, The Physics of the Quark-Gluon Plasma, Lecture Notes in Phys. 225 (1985), Springer-Verlag
9. R.C. Hwa, Phys. Rev. D32 (1985) 637
10. Y. Ivanov, I. Mishustin, L. Saratov, Nucl. Phys. A433 (1985) 619
11. S. Date, M. Gyulassy, and H. Sumiyoshi, Phys. Rev. D32 (1985) 619
    W. Busza and A.S. Goldhaber, Phys. Lett. 139B (1984) 235
    J. Hüfner and A. Klar, Phys. Lett. 145B (1984) 167
    L.P. Csernai and J.I. Kapusta, Phys. Rev. D29 (1984) 2664; D31 (1985) 2795;
12. G. Giacomelli and M. Jacob, Phys. Rep. 55 (1979) 1
13. R.B. Clare and D. Strottman, Phys. Reports 141 (1986) 177
14. H.W. Barz, B. Kämpfer, L.P. Csernai and B. Lukács, Phys. Lett. 143B (1984) 3334
15. H.W. Barz, B. Kämpfer, L.P. Csernai and B. Lukács, Phys. Rev. C31 (1985) 286
16. H. Stöcker and W. Greiner, Phys. Rep. 137 (1986) 277

R. Stock, Phys. Rep. 135 (1986) 259

17. L.P. Csernai, Phys. Rev. D29 (1984) 1945

18. L.P. Csernai, I. Lovas, J. Maruhn, A. Rosenhauer, J. Zimanyi and W. Greiner, Phys. Rev. C26 (1982) 149

19. B. Kämpfer, H.W. Barz, L. Münchow and B. Lukács, KFKI report, 85-77 (1985) and Acta Phys. Pol. B17 (1986) 685

20. P.R. Subramanian, H. Stöcker, and W. Greiner, University of Frankfurt preprint UFTP 169/1986

Figure Captions

Figure 1 - Density profiles of the target slab solid lines and the projectile slab (dashed lines) seen in the lab system at different lab times for E/A = 20 GeV and D is given by eq. (2.6).

Figure 2 - Comparison of the trajectories of the state variables n and T for a slab on slab collision for two different relaxation times (a) τ=1 fm/c and (b) τ=0.1 fm/c for the phase transiton to the quark-gluon plasma. Results using the coupling (2.6) are shown for E_{lab}=10 GeV (dotted lines), 40 GeV (solid lines) and 160 GeV (dashed lines). The numbers give the fractions of nuclear matter at the turning point.

Figure 3 - Maximum of energy density obtained in a slab on slab collision as a function of the bombarding energy. The dashed/solid lines are obtained using a diffusion constant given by eq. (2.5/2.6) respectively.

Figure 4 - Fraction of energy (in percent) transformed into intrinsic energy as a function of the bombarding energy. The dashed solid lines are btained using a diffusin constant given by eqs. (2.5-2.6) respectively.

Figure 5 - Maximum of energy density c (left scale) and particle density n (right scale) as a function of the slab thickness d calculated with D=1.2 GeV fm^2 and a relaxation time of τ=0.1 fm/c for different bombarding energies.

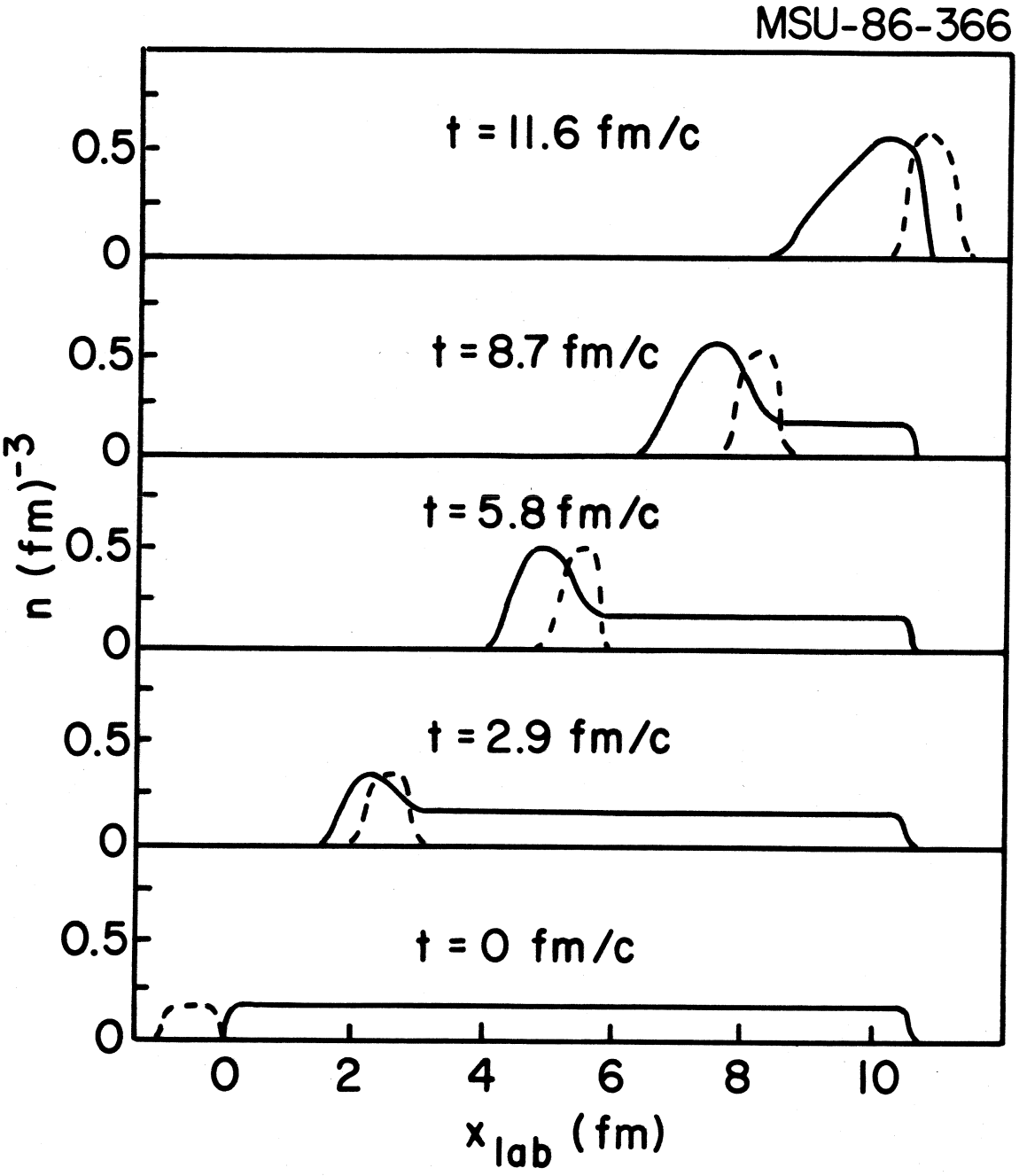
MSU-86-366
t = 11.6 fm/c
t = 8.7 fm/c
t = 5.8 fm/c
t = 2.9 fm/c
t = 0 fm/c
0.5
0
n (fm)^-3
0
2
4
6
8
10
x lab (fm)

Figure 1

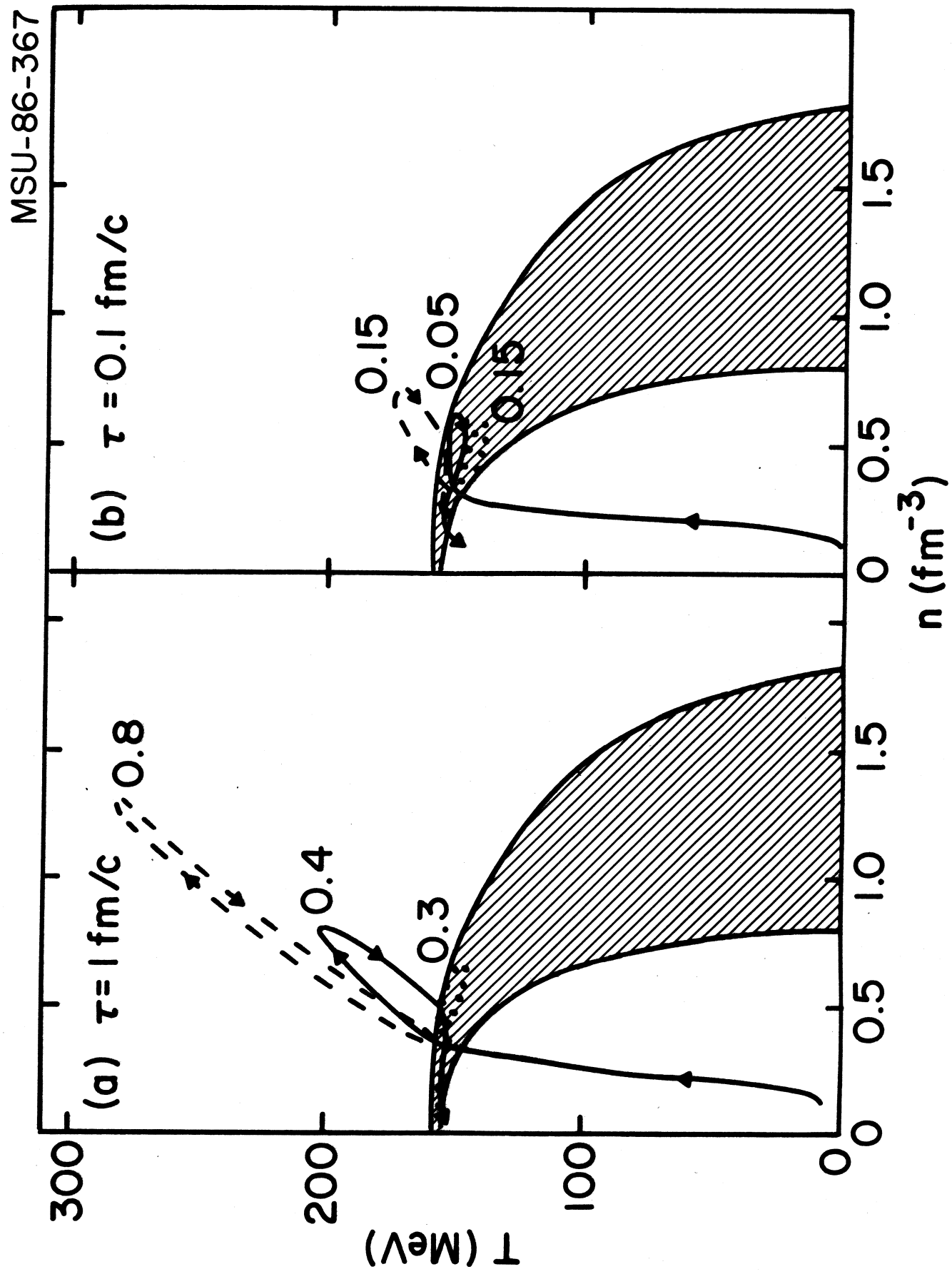
MSU-86-367
(b) τ = 0.1 fm/c
0.15
0.05
0.15
(a) τ = 1 fm/c
0.8
0.4
0.3
T (MeV)
300
200
100
0
0.5
1.0
1.5
n (fm⁻³)

Figure 2

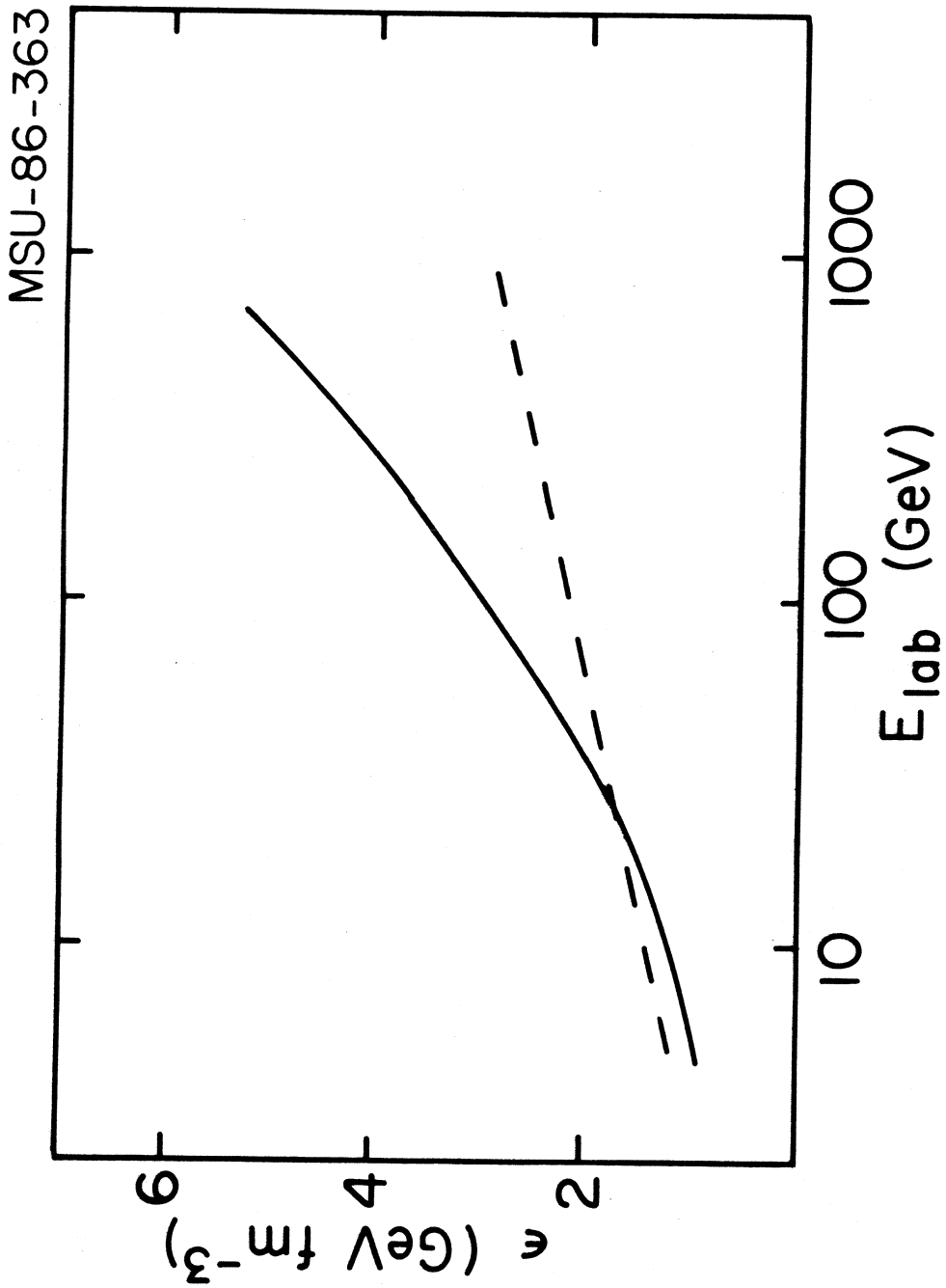

Figure 3

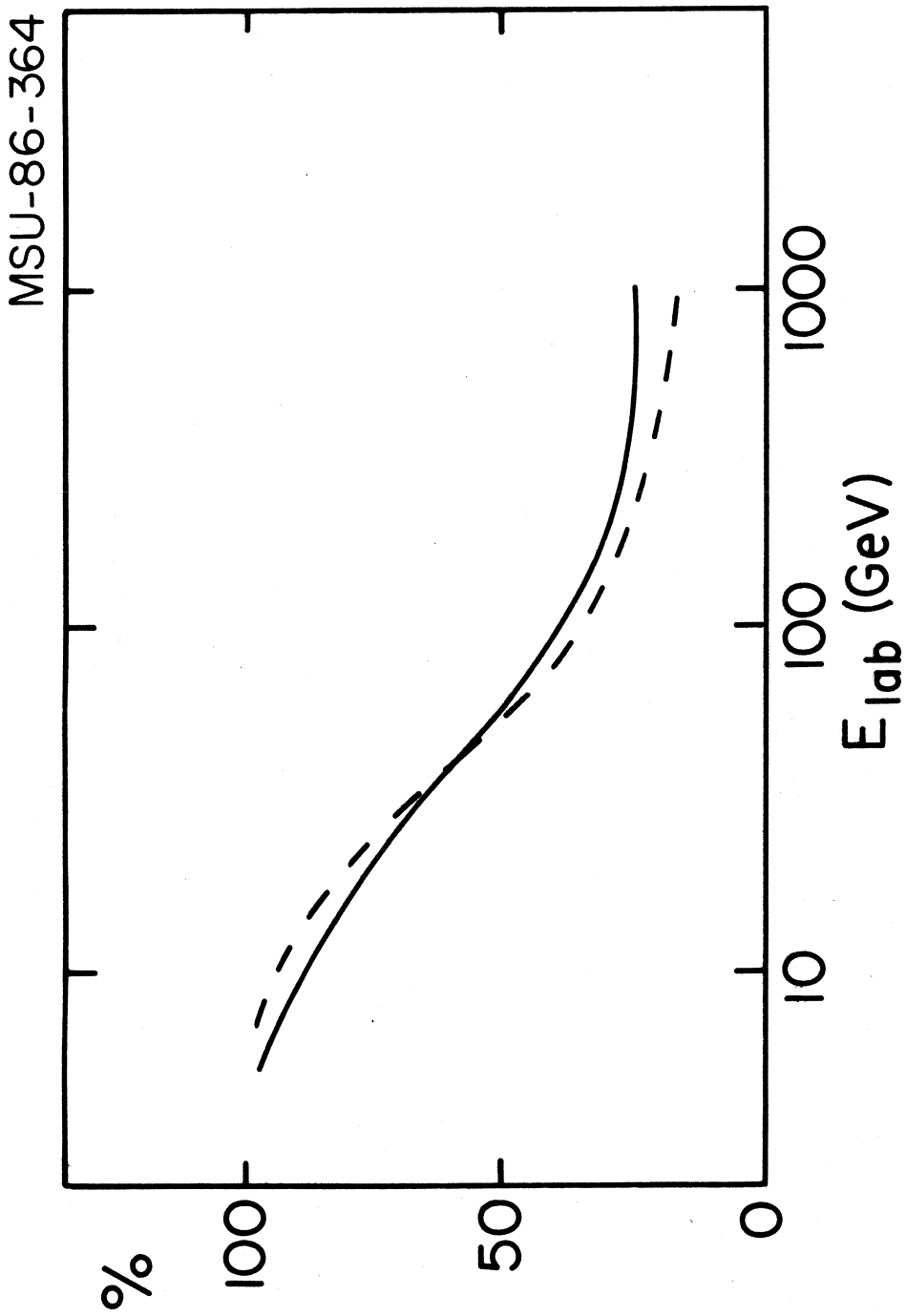

Figure 4

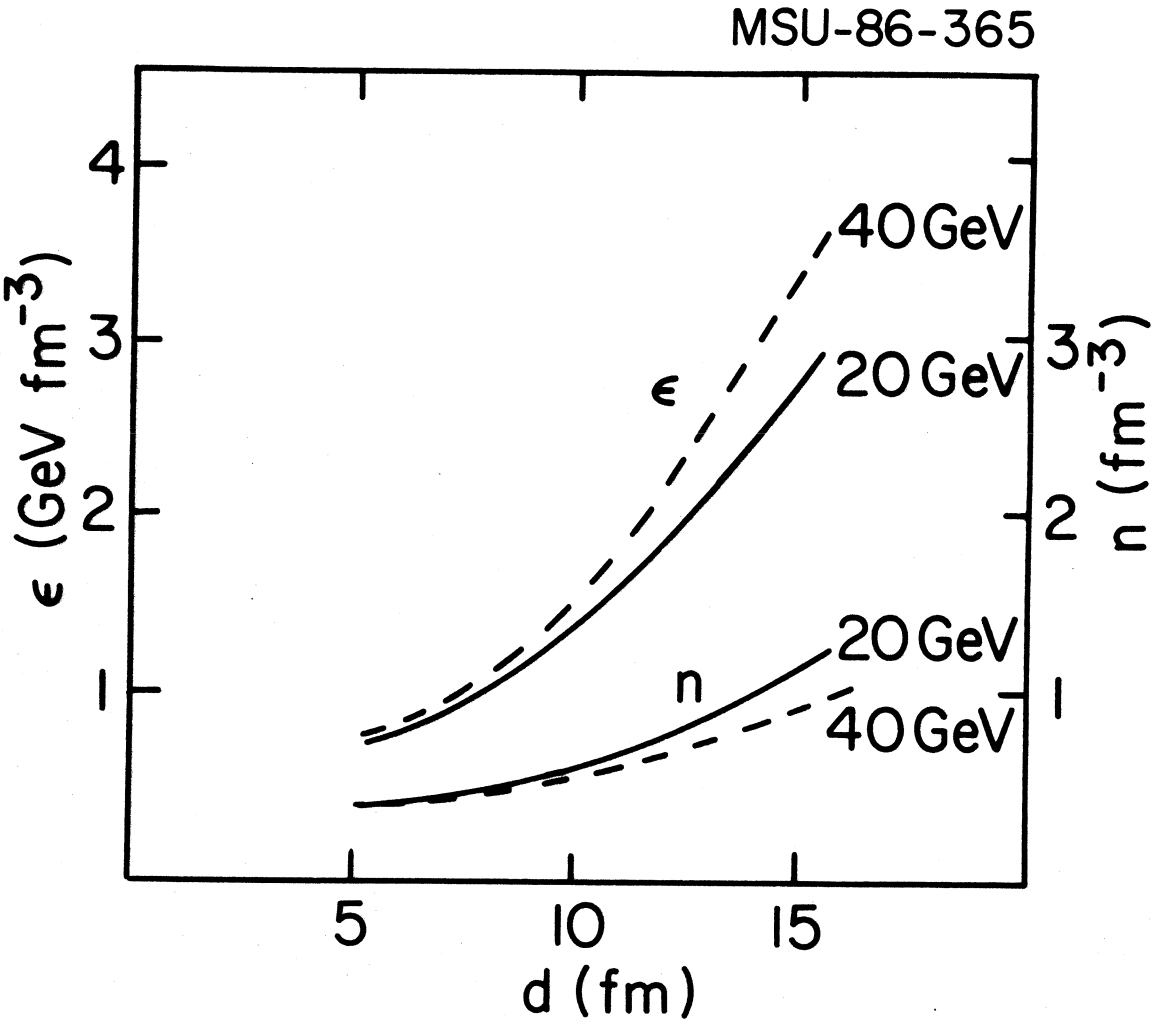
MSU-86-365
ε (GeV fm⁻³)
n (fm⁻³)
d (fm)
40 GeV
20 GeV
ε
20 GeV
n
40 GeV
1
2
3
4
5
10
15

Figure 5